Supporting Information

Regulation of Polysulfide Adsorption and LiF-rich Interface Chemistry to Achieve High-performance PEO-based Lithium-Sulfur Battery

Huanhuan Duan [a], Leiping Liao [a], Ran Bi [a], Yuanfu Deng [a,b,*], Guohua Chen [c]

[a] *Guangdong Provincial Key Laboratory of Fuel Cell Technology, School of Chemistry and Chemical Engineering, South China University of Technology, Guangzhou, 510640, Peoples R China;*

[b] *Guangdong Provincial Research Center of Electrochemical Energy Engineering, South China University of Technology, Guangzhou, 510640, Peoples R China;*

[c] *School of Energy and Environment, City University of Hong Kong, Tat Chee Avenue, Kowloon, Hong Kong, Peoples R China.*

Corresponding author.

E-mail address: chyfdeng@scut.edu.cn (Y.F. Deng).

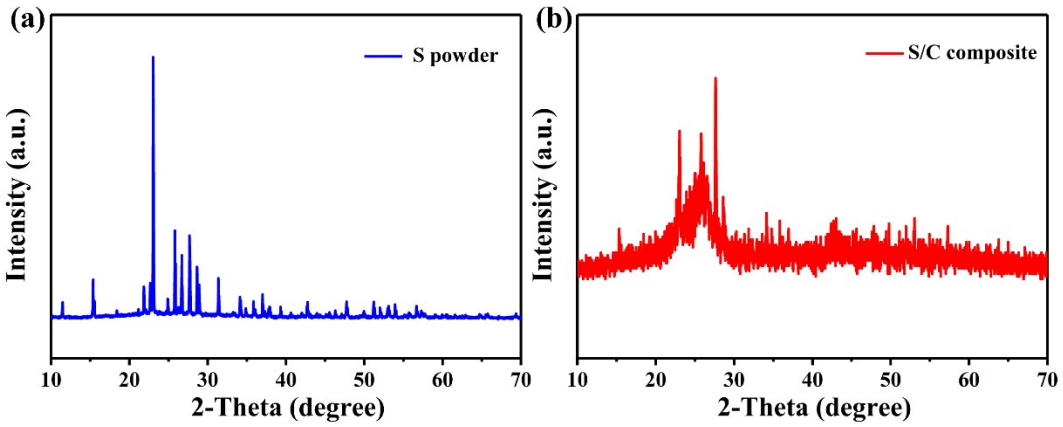

Figure S1. XRD curves of (a) S powder and (b) S/C composite.

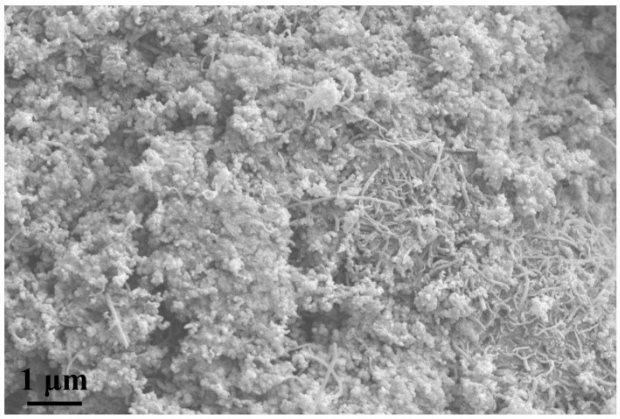

Figure S2. SEM image of S/C composite.

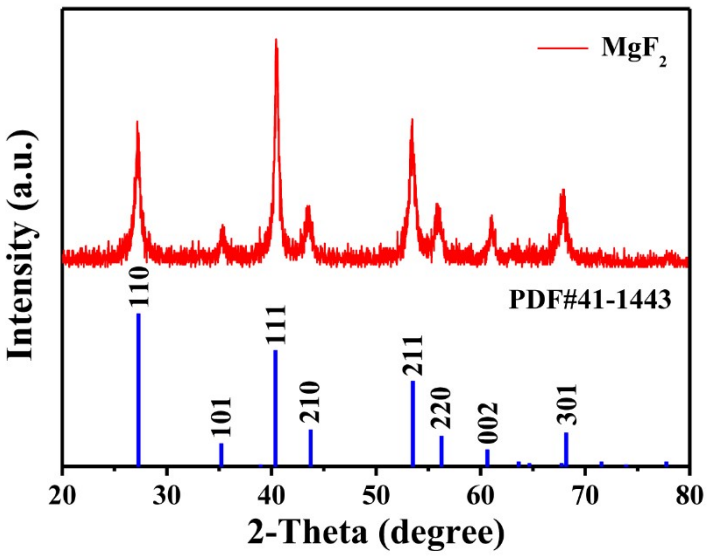

Figure S3. The XRD pattern of MgF_2 nanoparticles and corresponding crystal planes.

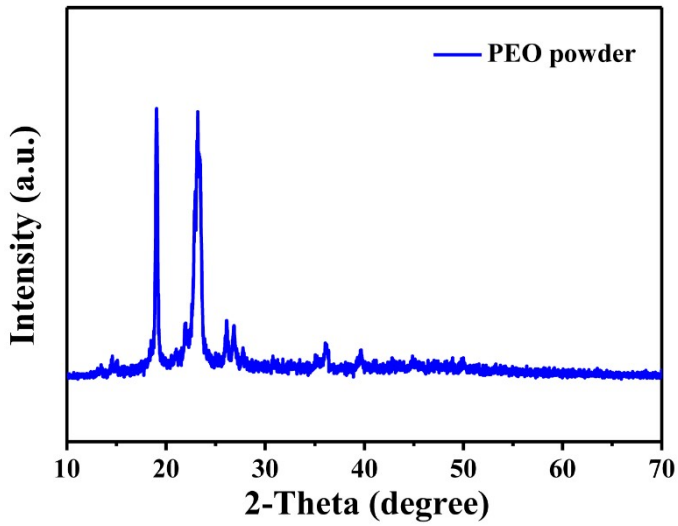

Figure S4. XRD curve of PEO powder.

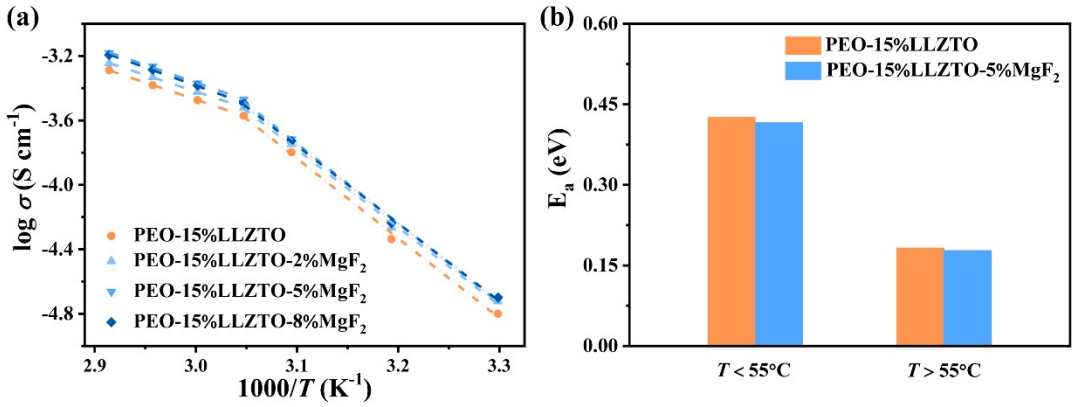

Figure S5. (a) Ionic conductivities for the PEO-15%LLZTO-x%MgF_2 (x = 0, 2, 5, and 8) SSEs; (b) The activation energy calculated from the ionic conductivity curves of PEO-15%LLZTO and PEO-15%LLZTO-5%MgF_2 SSEs at different sections (30 - 55℃ and 55 - 70℃).

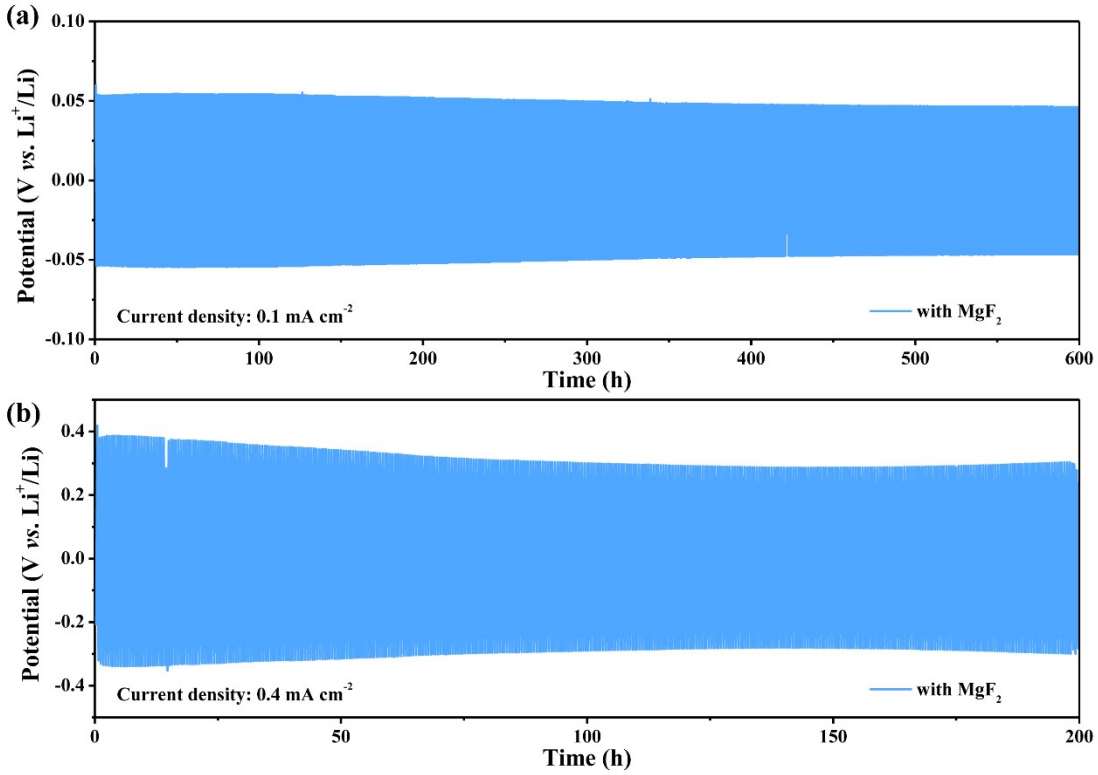

Figure S6. The electrochemical performances of Li/Li symmetrical batteries with the PEO-15%LLZTO-5%MgF_2 SSE at 50℃ with current densities of (a) 0.1 mA cm^{-2} and (b) 0.4 mA cm^{-2}.

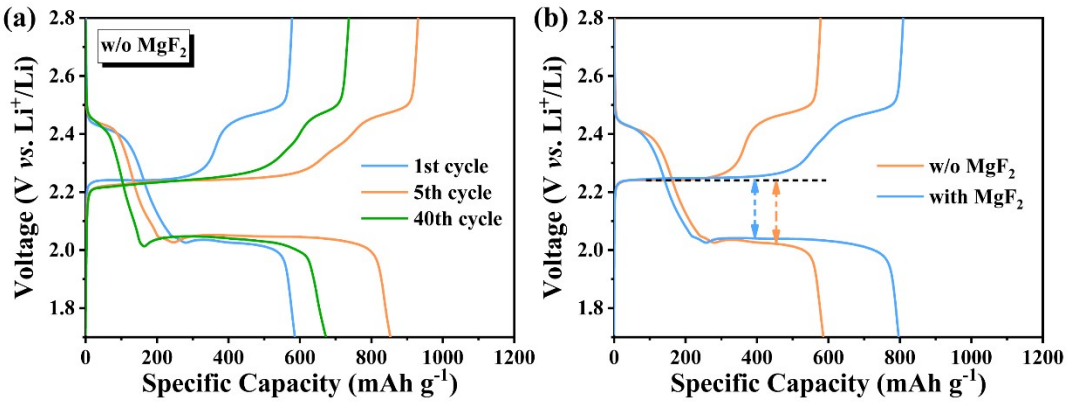

Figure S7. (a) The charge-discharge curves of the ASSLSB with the PEO-15%LLZTO SSE under 50℃ at 0.05 C; (b) Comparisons of the charge-discharge curves for the ASSLSBs assembled by the SSEs with or without the MgF_2 additive under 50℃ at 0.05 C.

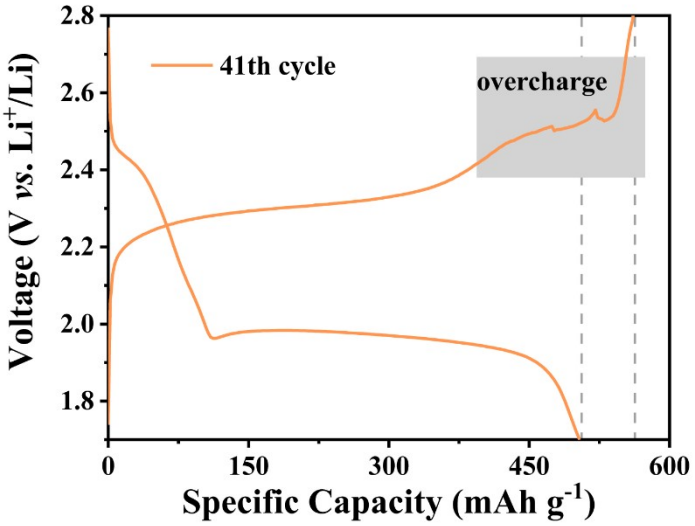

Figure S8. The charge-discharge curves of the ASSLSB with the PEO-15%LLZTO SSE under 60℃ at a current density of 0.2 C.

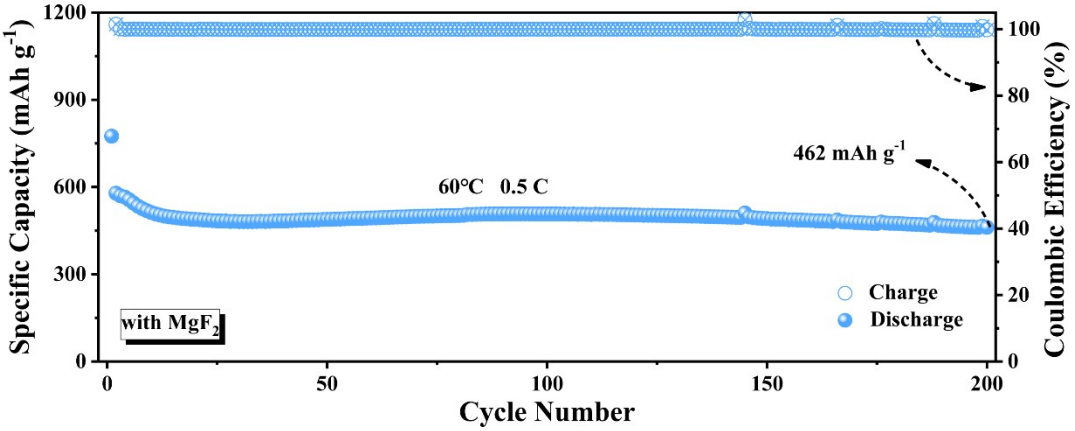

Figure S9. Long-term cycle performance of ASSLSBs with the PEO-15%LLZTO-5%MgF_2 SSE under 60℃ at 0.5 C.

Table S1. Electrochemical performances of lithium-sulfur batteries with PEO-based solid-state electrolytes.

Cathode	S loading / mg cm^{-2}	S content / %	Electrolyte	*T* / °C	Current density	Capacity / mAh g^{-1} (cycle number)	Retention rate / %	Coulombic efficiency / %	Ref.
S@CTT/MXene	0.6	25	PEO-LiTFSI-PE	55	0.12 C	584 (100)	—	—	[1]
S-CNTs	0.28	42	Al_2O_3 modified PEO	60	0.1 C 0.2 C	640 (120) 780 (100)	45.2 82.5	98.0 98.9	[2]
S/BC	1.2	48	PEO/PGA-LiTFSI-Py_{13}TFSI	50	0.2 C	541 (100)	89	—	[3]
S-super P-PEO/LiTFSI	0.6	40	C-S-E/4000k	55	0.2 C	768 (100)	83	98.0	[4]
S/BP-2000	—	—	PEO-PAN-LiTFSI	70	0.1 C	766 (75)	61.8	~100.0	[5]
Li_2S@TiS_2-super P-PEO/LiTFSI	0.2-1.2	—	PI@PEO/LiTFSI	80	0.8 C	333 (150)	68	98.6	[6]
Li_2S@AQT-PEO/LiTFSI	0.2-0.7	—	PE@PEO/LiTFSI	60	0.1 C	878 (30)	87.9	98.9	[7]

S/KB	0.5	56	PEO-LiTFSI-LLZTO with CGS interlayer	60	0.2 C	799 (50)	95.9	85.0	[8]
S	0.41	70	PEO-LiTFSI-LLZTO	45	~0.07 C	440 (50)	136.6	97.1	[9]
				55		168 (50)	35	90.5	
				65		106 (50)	~10	89.7	
				75		117 (50)	~10	88.6	
S-KB-CNT-PEO/LiTFSI	0.5	50	PFA|PEO	60	~0.06 C	627 (100)	53.6	98.0	[10]
S/KB-CB-CNT	**0.5**	**45**	**PEO-LLZTO-5%MgF_2**	**50**	**0.05 C**	**874 (40)**	**90**	**98.5**	**This work**
				60	**0.2 C**	**780 (40)**	**98**	**99.7**	
				60	**0.2 C**	**732 (60)**	**92**	**98.3**	

Note: for the cathode with S as active material, 1 C = 1675 mA g^{-1}; for the cathode with Li_2S as active material, 1 C = 1166 mA g^{-1}. "—" indicates that the data is not given.

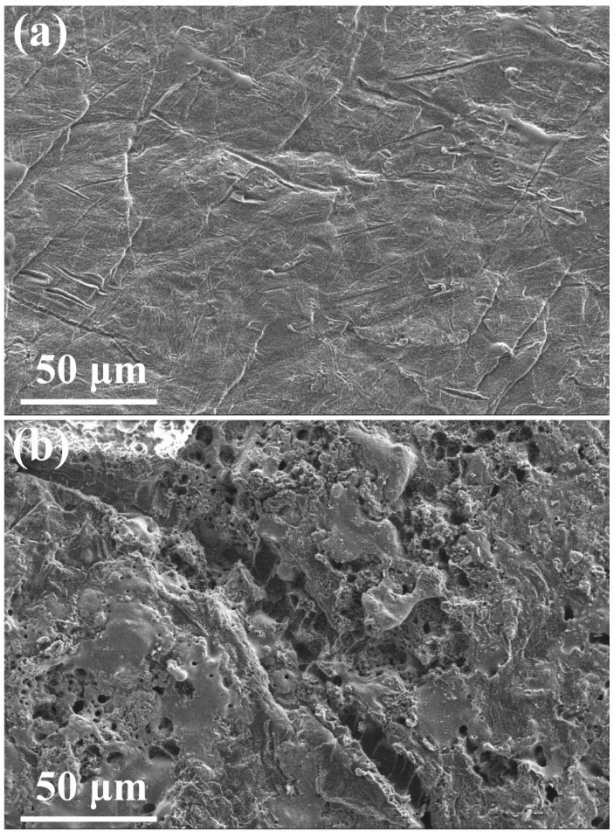

Figure S10. (a) SEM image of the cycled lithium metal surface from the battery with the PEO-15%LLZTO-5%MgF_2 SSE; (b) SEM image of cycled lithium metal surface from the battery with the PEO-15%LLZTO SSE.

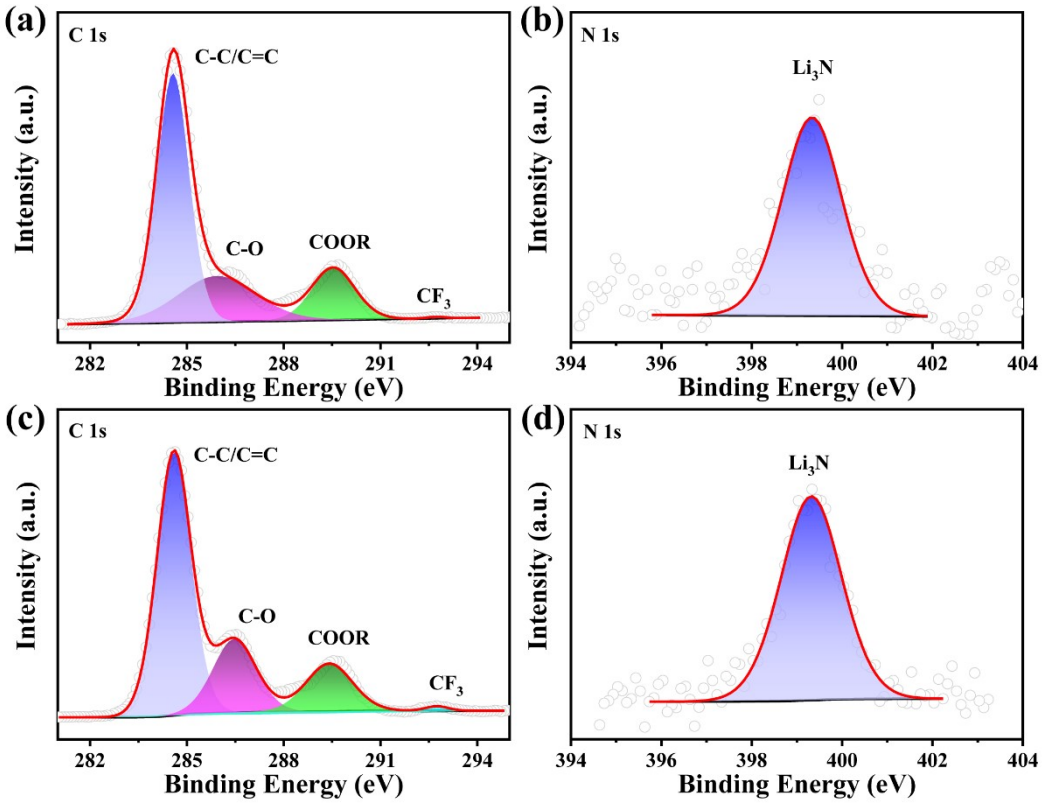

Figure S11. XPS spectra of the cycled lithium metal surface from the battery with the PEO-15%LLZTO-5%MgF_2 SSE: (a) C 1s; (b) N 1s; and those with PEO-15%LLZTO SSE: (c) C 1s; (d) N 1s.

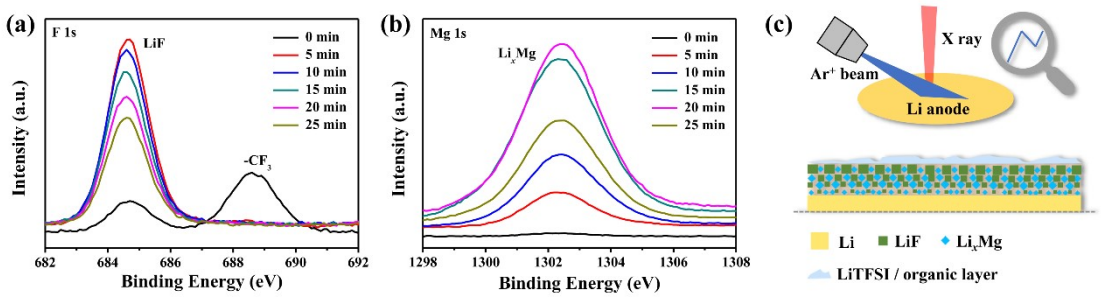

Figure S12. Comparison of XPS spectra of (a) F 1s and (b) Mg 1s before and after sputtering under the same conditions (Ar^+, 5 keV, 3 mm×3 mm); (c) The schematics of Ar^+ sputtering process and SEI model (The LiF and Li_xMg alloy layers are used as the main components; other components such as lithium sulfide and lithium nitride are not considered here).

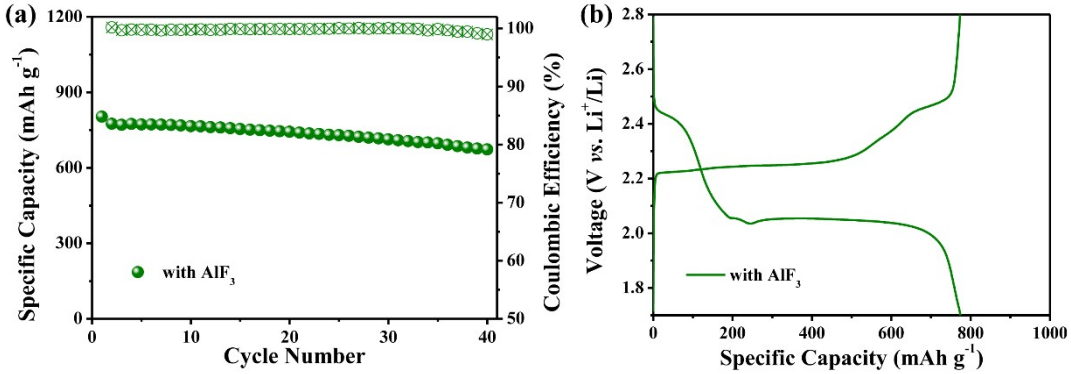

Figure S13. (a) Cycle performance and (b) the corresponding charge-discharge curves of the ASSLSB with the PEO-15%LLZTO-5%AlF_3 SSE under 60℃ at a current density of 0.2 C.

We used the same method to prepare the solid-state electrolyte (denoted as PEO-15%LLZTO-5%AlF_3) using AlF_3 as an additive. The ASSLSB's electrochemical performance at 0.2 C and 60℃ is investigated. As shown in **Figure S13a**, the ASSLSB shows a high discharge specific capacity of 812 mAh g^{-1}, accompanied by a high Coulombic efficiency of about 100%. In addition, this battery also has a lower polarization voltage of 0.20 V (**Figure S13b**). As we excepted, the AlF_3 additive shows a similar effect on modifying the PEO-based electrolyte with MgF_2, due to their similar properties.

References:

1 Y. Zhang, Y. Wu, Y. Liu and J. Feng, *Chem. Eng. J.*, 2022, **428**, 131040.

2 Y. Shi, Z. Fan, B. Ding, Z. Li, Q. Lin, S. Chen, H. Dou and X. Zhang, *J. Electroanal. Chem.*, 2021, **881**, 114916.

3 J. Li, H. Zhang, Y. Cui, H. Da, H. Wu, Y. Cai and S. Zhang, *Chem. Eng. J.*, 2023, **454**, 140385.

4 L. Wang, X. Yin, C. Jin, C. Lai, G. Qu and G. W. Zheng, *ACS Appl. Energy Mater.*, 2020, **3**, 11540-11547.

5 J. Sheng, Q. Zhang, C. Sun, J. Wang, X. Zhong, B. Chen, C. Li, R. Gao, Z. Han and G. Zhou, *Adv. Funct. Mater.*, 2022, **32**, 2203272.

6 X. Gao, X. Zheng, J. Wang, Z. Zhang, X. Xiao, J. Wan, Y. Ye, L. Y. Chou, H. K. Lee, J. Wang, R. A. Vila, Y. Yang, P. Zhang, L. W. Wang and Y. Cui, *Nano Lett.*, 2020, **20**, 5496-5503.

7 X. Gao, X. Zheng, Y. Tsao, P. Zhang, X. Xiao, Y. Ye, J. Li, Y. Yang, R. Xu, Z. Bao and Y. Cui, *J. Am. Chem. Soc.*, 2021, **143**, 18188-18195.

8 Y. Liu, H. Liu, Y. Lin, Y. Zhao, H. Yuan, Y. Su, J. Zhang, S. Ren, H. Fan and Y. Zhang, *Adv. Funct. Mater.*, 2021, **31**, 2104863.

9 Y.-X. Song, Y. Shi, J. Wan, S.-Y. Lang, X.-C. Hu, H.-J. Yan, B. Liu, Y.-G. Guo, R. Wen and L.-J. Wan, *Energy Environ. Sci.*, 2019, **12**, 2496-2506.

10 Y. An, Y. Cheng, S. Wang and J. Yu, *ACS Appl. Energy Mater.*, 2022, **5**, 2786-2794.